Magneto-Hemodynamic Flow in a Two-Sided Lid-Driven Cavity

Padmini Priyadarshini Sivaraj

[1]

November 24, 2019

ABSTRACT

An incompressible, laminar, non-Newtonian, magnetohydrodynamic solver, called nonNewtonianMHDFoam, is implemented in OpenFOAM. The effects of the magnetic field on the blood flow in a two-sided lid-driven square cavity with anti-parallel wall motion is studied using the nonNewtonianMHDFoam.
The flow is investigated at four different Stuart number (N = 0, 1, 10, 50) as Newtonian and non-Newtonian fluid. The viscosity of the blood is assumed to follow the power-law model.
The results from the simulations are compared with Kefayati (2014) for validation. It is observed that the magnetic field can destabilise and break the main core vortex into many; and when the blood is treated as Newtonian, the influence of magnetic field on the flow is comparatively less than when it is assumed to be a non-Newtonian fluid.

Key words. MHD – Cavity – Non-Newtonian – OpenFOAM

1. Introduction

The study of blood flow in the human body is integral in the branch of Biofluid Mechanics. Understanding the influences of forces due to blood flow and its effect on the blood vessel wall is crucial in the study of the cardiovascular system and the related diseases.

Since blood is an electrically conducting fluid, it interacts with the magnetic field. Such type of interaction is prevalent in cardiac MRI. Due to the interaction of the magnetic field with the blood flow in the aorta, an electrical potential is induced, which increase the T-wave in the electrocardiogram. This magnetohydrodynamic effect during cardiac MRI was investigated by Martin et al. (2012). Magneto-hemodynamic is the branch of fluid mechanics which deals with the study of the blood flow in the presence electromagnetic field.

The driven cavity flow is a benchmark problem in fluid dynamics, as it gives insight into some important aspects of the fluid flow like the vortexes formation, the structure of the flow circulation zone, and the instability.

Kefayati (2014) studied the non-Newtonian fluid flow in a two-sided lid-driven cavity under the presence of the magnetic field using the Finite difference Lattice Boltzmann method. Kefayati (2014) also discussed the effect of Reynolds number, Stuart number, power index on the flow behaviour. Selimefendigil and Chamkha (2016) investigated the non-Newtonian, magnetohydrodynamics mixed convection of a lid-driven cavity with a corrugated bottom wall with an inclined magnetic field.

In this paper, a general incompressible, laminar, non-Newtonian, MHD solver is implemented in OpenFOAM. The simulation results for the blood flow are compared with Kefayati (2014) for validation and the flow behaviour at various Stuart number and power-law index is discussed.

2. Fluid model

The blood flow is modelled as a single-phase flow and both Newtonian and Non-Newtonian behaviours are investigated.

Blood is a non-Newtonian fluid: viscosity of blood varies based on the applied force. Power-law fluids link viscosity and strain rate as follows,

$$\nu = K\dot{\gamma}^{n-1} \tag{1}$$

where n is the power-law index, and K is the consistency coefficient. When $n = 1$ the equation becomes Newtonian. The intensity of strain rate, $\dot{\gamma}$ is defined as follow,

$$\dot{\gamma} = \sqrt{2\bar{\bar{\Delta}} : \bar{\bar{\Delta}}} \tag{2}$$

where $\bar{\bar{\Delta}}$ is the rate of deformation $\frac{1}{2}(\nabla\mathbf{V}+(\nabla\mathbf{V})^T)$, the symmetric part of the tensor $\nabla\mathbf{V}$.

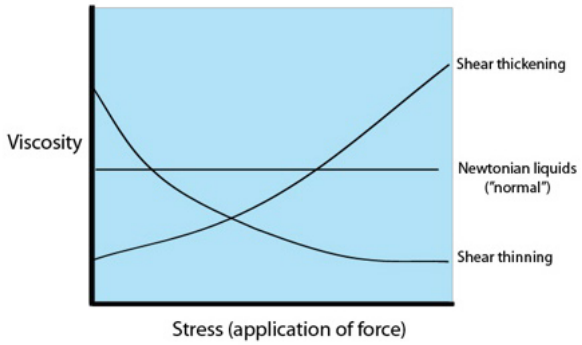

Fig. 1: Non-Newtonian fluid behaviour
Source: Science Learning Hub – Pokapū Akoranga Pūtaiao. (2010). Non-Newtonian fluids. Retrieved from www.sciencelearn.org.nz/resources/1502-non-newtonian-fluids

Blood is a shear-thinning fluid, i.e., viscosity decreases with an increase in strength of the applied force, hence, the power-law index,n for blood is less than one. OpenFOAM provides a limit for maximum and minimum value of viscosity, ν_{max} and ν_max, to avoid singularity in the calculation.

3. Problem definition

The geometry consists of a two-dimensional square duct of dimension $L \times L$ with two moving (top and bottom) and two stationary or fixed walls (left and right).

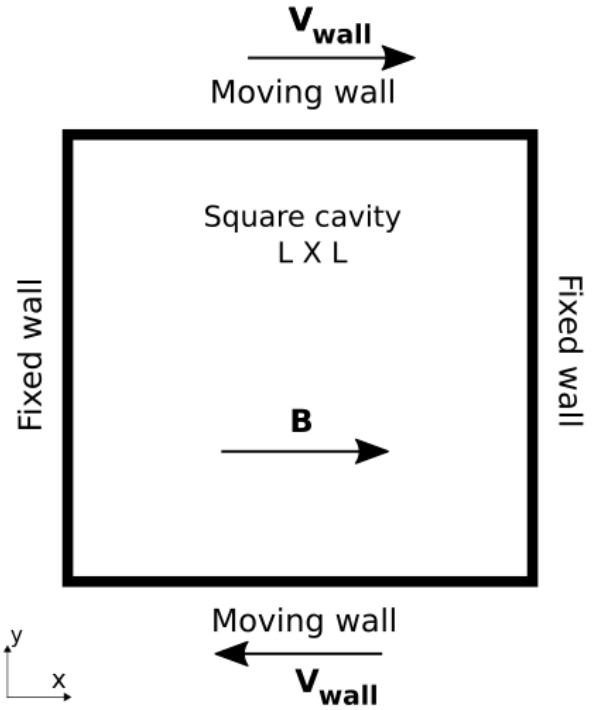

Fig. 2: Case Setup

The top and bottom walls are assumed to be moving with a velocity, V_{wall} in the opposite direction. The square cavity consists of an incompressible, non-Newtonian, electrically conducting fluid, whose thermophysical and electrical properties are listed in the table 2. A homogeneous and steady magnetic field of strength B is applied parallel to the moving wall axis. The walls are assumed to be perfectly conducting.

Table 1: Boundary conditions

	Pressure ($Pascal$)	Velocity (m/s)	Magnetic Field ($Tesla$)	pB ($Tesla\,m/s$)
Top walls	zero gradient	(V_x 0 0)	zero gradient	0
Bottom wall	zero gradient	($-V_x$ 0 0)	zero gradient	0
Fixed walls	zero gradient	(0 0 0)	zero gradient	0

Table 2: Thermophysical and Electrical properties of the working fluid

	Value	SI units
Density	800	kg/m^3
Consistency coefficient	0.004	kg/ms
Dynamic viscocity max	0.01	kg/ms
Dynamic viscocity min	1.00E-03	kg/ms
Power law index*	0.6 , 1	
Electrical conductivity	0.7	S/m
Magnetic constant	1.257E-06	H/m

*Simulations are run at two different power-law index, (n = 0.6, 1) either as non-Newtonian or Newtonian fluid.

4. Governing equation

The fundamental equation governing the incompressible, non-Newtonian, magnetohydrodynamic flow is given by the following equation.

1) Conservation of mass

$$\nabla \bullet \mathbf{V} = 0 \tag{3}$$

2) Conservation of momentum

$$\frac{\partial \mathbf{V}}{\partial t} + \nabla \bullet (\mathbf{VV}) - \nabla \bullet \tau - \nabla \bullet \left(\frac{1}{\mu_0 \rho}\mathbf{BB}\right) + \nabla\left(\frac{1}{2\mu_0\rho}B^2\right) = -\nabla P \tag{4}$$

3) Conservation of magnetic flux

$$\nabla \bullet \mathbf{B} = 0 \tag{5}$$

4) Magnetic induction equation

$$\frac{\partial \mathbf{B}}{\partial t} + \nabla \bullet (\mathbf{VB}) - \nabla \bullet (\mathbf{BV}) - \Delta\left(\frac{1}{\mu_0 \sigma}\mathbf{B}\right) = 0 \tag{6}$$

The viscous term is expanded as,

$$\nabla \bullet \boldsymbol{\tau} = \nabla \bullet \left[\nu \nabla \mathbf{V} + \nu (\nabla \mathbf{V})^T\right] = \nabla \bullet (\nu \nabla \mathbf{V}) + (\nabla \mathbf{V}) \bullet \nabla \nu \tag{7}$$

The term $(\nabla \mathbf{V}) \bullet \nabla \nu$ corresponds to the spatial variation of viscosity in non-Newtonian fluids.

5. Non-dimensional parameters

The Reynolds number, Hartmann number and Stuart number for non-Newtonian fluids are defined as follows:

1. Reynolds number

$$\frac{Inertial\,force}{Viscous\,force} = Re = \frac{\rho {V_c}^{2-n} {L_c}^{n}}{K} \tag{8}$$

2. Hartmann number

$$\frac{Electromagnetic\,force}{Viscous\,force} = Ha = B\sqrt{\frac{{L_c}^{n+1}\sigma}{{V_c}^{n-1}K}} \tag{9}$$

3. Stuart number

$$\frac{Electromagnetic\,force}{Inertial\,force} = N = \frac{Ha^2}{Re} \tag{10}$$

where L_c, V_c refers to the characteristic length and characteristic velocity respectively and in this case L_c = Dimension of the cavity and V_c = Velocity of the wall.

The nonNewtonianMHDFoam is a pressure-based solver. The magnetic induction method is implemented in a similar way to the existing MHD solver, the mhdFoam. The PISO algorithm is used to solve both Navier-Stokes and magnetic induction equation. Figure 3 shows the detailed flowchart.

6. Grid Independence

Grid independence study is conducted for two different meshes. The detail of the meshes are shown in the table.

	number of grids
Mesh no. 1	50×50
Mesh no. 2	150×150

From the graphs 4, it is observed that the velocity profile is in good agreement for different meshes. Mesh number 1 is used for further simulations.

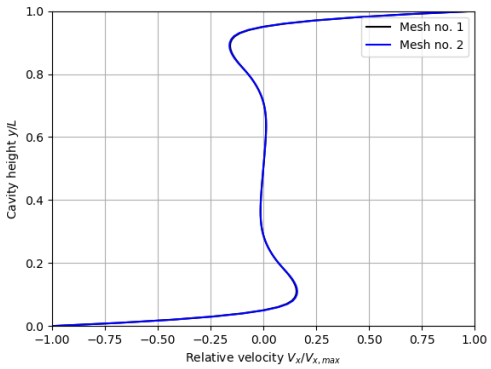

Fig. 4: Relative horizontal velocity component at x/L = 0.5

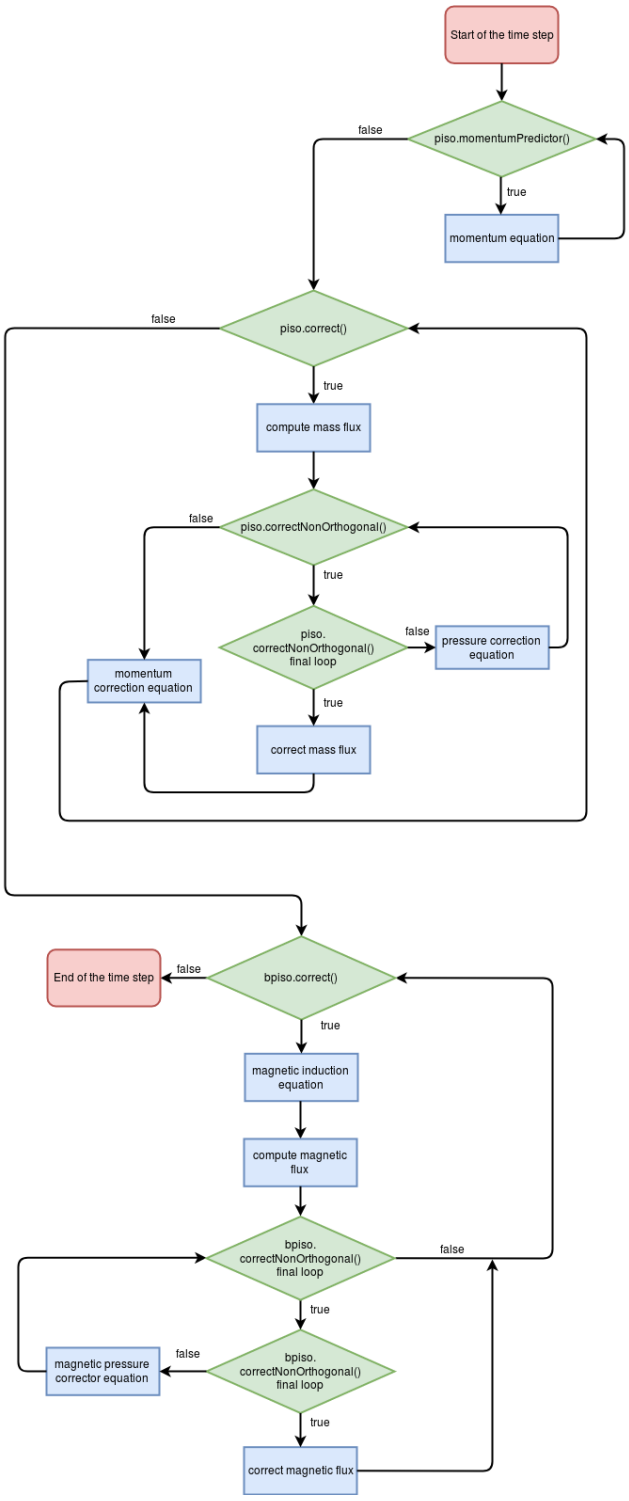

Fig. 3: nonNewtonianMHDFoam solver algorithm

7. Result and Discussion

The simulations are at four different Stuart number (N = 0, 1, 10, 50) treating the flow as Newtonian or non-Newtonian. The streamline patterns are visualised using the paraView tool "streamtracer" and the graphs are plotted using Python's matplotlib plotting library. The letters "C" and "A" on the streamline pattern figures 5 and 6 represent clockwise and anti-clockwise vortexes respectively.

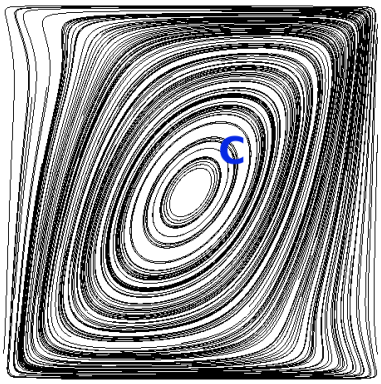

(a) $Re = 100, N = 0, non - Newtonian$

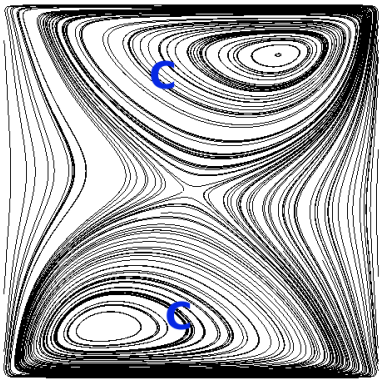

(b) $Re = 100, N = 1, non - Newtonian$

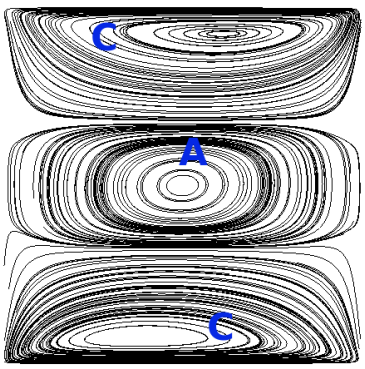

(c) $Re = 100, N = 10, non - Newtonian$

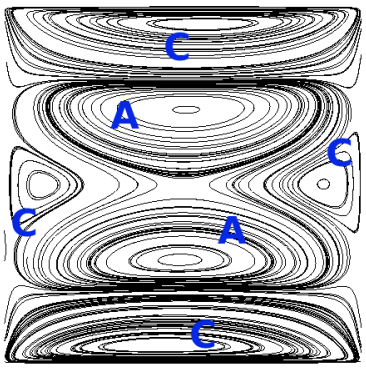

(d) $Re = 100, N = 50, non - Newtonian$

Fig. 5: Streamlines pattern for different Stuart number

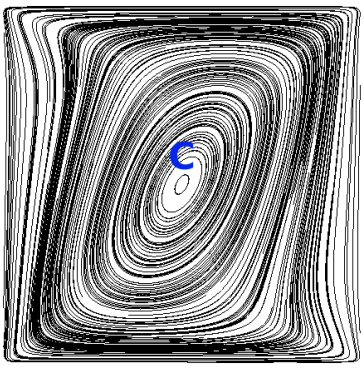

(a) $Re = 100, N = 0, Newtonian$

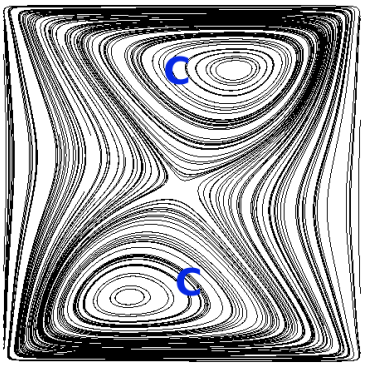

(b) $Re = 100, N = 1, Newtonian$

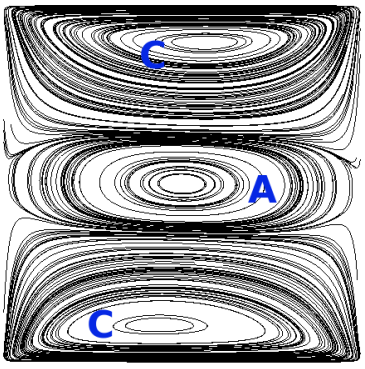

(c) $Re = 100, N = 10, Newtonian$

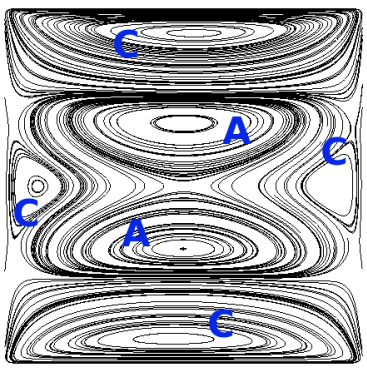

(d) $Re = 100, N = 50, Newtonian$

Fig. 6: Streamlines pattern for different Stuart number

Figure 5 show the ability of the magnetic field to break the main core vortex into many when its strength is increased. The number of the circulation zone increases with increasing Stuart number. When increased from $N = 0$ to $N = 1$, 5b, the circulation zone splits into two, a clockwise vortex near the bottom lid and another clockwise vortex near the top lid and these two vortexes are split symmetrically; on further increase to $N = 10$, 5c, the three circulation zone formation occurs: a clockwise vortex near the bottom lid and a clockwise vortex near the top lid and another newly formed anticlockwise vortex at the middle; at the Stuart number of value 50, 5d, a much more complex system of vortexes develops, the middle vortex at $N = 10$ splits symmetrically into two anti-clockwise vortexes, a clockwise vortex near the bottom, a clockwise vortex near the top, and two additional clockwise vortexes near the left and right wall. However, in the work done by Kefayati (2014), there exist two additional weak vortex near the left and right wall at $N = 1$, and the two clockwise vortex near left and right wall at $N = 50$ are absent.

The figure 7 shows the relative horizontal velocity component profile taken along the cavity height at mid-width for various Stuart number from the OpenFOAM simulation, plotted against the results from Kefayati (2014). Figure 7 shows a fair agreement of OpenFOAM simulation result with the numerical investigation conducted by Kefayati (2014) using FDLBM.

It can be observed from the velocity profile at $N = 0$ in figure 7 that the positive-valued velocity near the top wall decreases slowly up to a certain distance away from the top wall, followed by a linear variation in the main core region. At the centre of the cavity, the velocity approaches zero, which is in agreement with the streamline pattern shown in the figure as this region corresponds to the centre of the main core. The velocity then tends towards the negative velocity of the bottom wall.

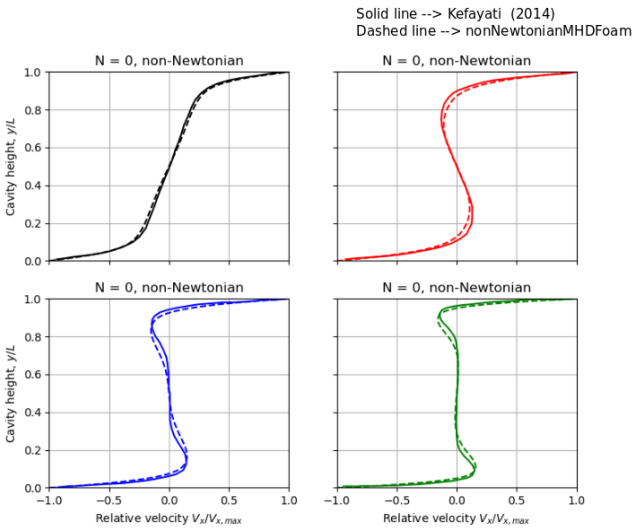

Fig. 7: Velocity, $\mathbf{V_x}$ at mid width

The velocity profile is S-shaped at $N = 1$. This could be attributed to the clockwise vortex near the bottom lid and the clockwise vortex near the top lid: near the top lid, the velocity is positive due to the positive velocity of the top lid, but at slightly later distance away from the top lid, the velocity lean towards a negative value then towards zero as we move towards the centre of the cavity. This pattern is due to the presence of clockwise vortex in the upper half of the cavity. The clockwise vortex in the lower half of the cavity gives rise to an inverse pattern: a zero velocity at the center, which belongs to the meeting point of the two vortex where the negative velocity of top clockwise vortex and positive value of bottom clockwise vortex cancels each other; followed by positive valve, due to the lower half of the clockwise vortex; finally ending in negative value, which is the no-slip condition existing near the wall.

In the graph which corresponds to the velocity profile at $N = 10$, it can be seen that the positive peak due to the clockwise vortex is shifted slightly towards the top wall as the vortex is squeezed to the top due to the formation of the third vortex in the middle. The same can be said to the negative peak at the bottom. This translation of peaks is further accentuated in the graph which corresponds to $N = 50$. The appearance of further vortexes suppresses the strength of the neighbouring vortexes resulting in an almost perpendicular line placed at $V_x = 0$ seen in the near-middle region of the cavity at $N = 10$ and $N = 50$.

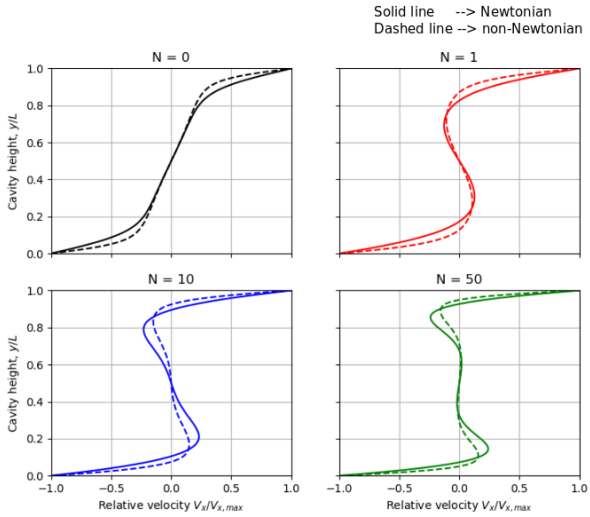

Fig. 8: Velocity, $\mathbf{V_x}$ at mid width

It is evident from the figure 6 and 5 that when blood is treated as Newtonian fluid i.e., $n = 1$, the vortexes shift towards the mid-line, $x/L = 0$, and the vortexes translates slightly towards the centre of the cavity. These effects are also evident in the graphs 8. When the Stuart number is increased, the difference in the translation of vortexes towards wall becomes less, but the difference in the magnitude of the peak becomes more pronounced.

Another noticeable difference between the Newtonian and non-Newtonian fluid treatment is that the strength of the vortex is relatively less in the non-Newtonian fluid model than the Newtonian fluid model. In figure 8 the magnitude of the peak for Newtonian fluid is relatively less than the magnitude of the peak for non-Newtonian fluid. In the figure 8, the green curve which corresponds to the velocity profile at $N = 50$, the magnitude of the peak on the dotted line is higher than the magnitude of the peak on the solid line. The strength of the vortex becomes high when the power-law index is increased, meaning the influence of the magnetic field on the flow weakens when the power-index increases. In other words, the magnetic field influences the blood flow less than it normally would if the fluid is treated as Newtonian.

8. Tools used

Mesh generator: blockMesh
Plot generator: Matplotlib, python
Graphic editor: Inkscape
Flowchart editor: Draw.io
Latex editor: Overleaf

References

Kefayati, G. R. (2014). Fdlbm simulation of magnetic field effect on non-newtonian blood flow in a cavity driven by the motion of two facing lids. *Powder technology*, 253:325–337.

Martin, V., Drochon, A., Fokapu, O., and Gerbeau, J.-F. (2012). Magnetohemodynamics in the aorta and electrocardiograms. *Physics in Medicine & Biology*, 57(10):3177.

Selimefendigil, F. and Chamkha, A. J. (2016). Magnetohydrodynamics mixed convection in a lid-driven cavity having a corrugated bottom wall and filled with a non-newtonian power-law fluid under the influence of an inclined magnetic field. *Journal of Thermal Science and Engineering Applications*, 8(2):021023.

Nomenclature

$\dot{\gamma}$	Strain rate
$\mathbf{B_0}$	Applied magnetic field, $Tesla$
$\mathbf{B}$	Total magnetic field, $Tesla$
$\mathbf{V}$	Velocity, m/s
μ	Dynamic viscosity, kg/ms
μ_0	magnetic constant, H/m
ν	Kinematic viscosity, m^2/s^2
ρ	Density, kg/m^3
σ	Electrical conductivity, S/m
Ha	Hartmann number
K	consistency coefficient, kg/ms
L	Length and height of the cavity, m
N	Stuart number
P	Pressure, N/m^2
Re	Reynolds number
V_{wall}	Velocity of the wall, m/s
x, y	Cartesian coordinates
n	Power-law index

Appendix A: nonNewtonianMHDFoam solver detail

```
/*---------------------------------------------------------------------------*\
  =========                 |
  \\      /  F ield         | OpenFOAM: The Open Source CFD Toolbox
   \\    /   O peration     |
    \\  /    A nd           | Copyright (C) 2011-2016 OpenFOAM Foundation
     \\/     M anipulation  |
-------------------------------------------------------------------------------
License
    This file is part of OpenFOAM.

    OpenFOAM is free software: you can redistribute it and/or modify it
    under the terms of the GNU General Public License as published by
    the Free Software Foundation, either version 3 of the License, or
    (at your option) any later version.

    OpenFOAM is distributed in the hope that it will be useful, but WITHOUT
    ANY WARRANTY; without even the implied warranty of MERCHANTABILITY or
    FITNESS FOR A PARTICULAR PURPOSE. See the GNU General Public License
    for more details.

    You should have received a copy of the GNU General Public License
    along with OpenFOAM. If not, see <http://www.gnu.org/licenses/>.

Application
    nonNewtonianIcoFoam

Description
    Transient solver for incompressible, laminar, MHD flow of non-Newtonian fluids.

\*---------------------------------------------------------------------------*/

#include "fvCFD.H"
#include "singlePhaseTransportModel.H"
#include "pisoControl.H"

// * * * * * * * * * * * * * * * * * * * * * * * * * * * * * * * * * * * * * //

int main(int argc, char *argv[])
{
    #include "postProcess.H"

    #include "setRootCase.H"
    #include "createTime.H"
    #include "createMeshNoClear.H"
    #include "createControl.H"
    #include "createFields.H"
    #include "initContinuityErrs.H"


    // * * * * * * * * * * * * * * * * * * * * * * * * * * * * * * * * * * * * //

    Info<< "\nStarting time loop\n" << endl;

    while (runTime.loop())
    {
        Info<< "Time = " << runTime.timeName() << nl << endl;

        #include "CourantNo.H"

        fluid.correct();

        {

        // Momentum predictor

        fvVectorMatrix UEqn
```

```
  (
      fvm::ddt(U)
    + fvm::div(phi, U)
    - fvm::laplacian(fluid.nu(), U)
    - (fvc::grad(U) & fvc::grad(fluid.nu()))
    - fvc::div(phiB, 2.0*DBU*B)
    + fvc::grad(DBU*magSqr(B))
  );

  if (piso.momentumPredictor())
  {
      solve(UEqn == -fvc::grad(p));
  }

  // --- PISO loop
  while (piso.correct())
  {
      volScalarField rAU(1.0/UEqn.A());
      volVectorField HbyA(constrainHbyA(rAU*UEqn.H(), U, p));
      surfaceScalarField phiHbyA
      (
          "phiHbyA",
          fvc::flux(HbyA)
        + fvc::interpolate(rAU)*fvc::ddtCorr(U, phi)
      );

      adjustPhi(phiHbyA, U, p);

      // Update the pressure BCs to ensure flux consistency
      constrainPressure(p, U, phiHbyA, rAU);

      // Non-orthogonal pressure corrector loop
      while (piso.correctNonOrthogonal())
      {
          // Pressure corrector

          fvScalarMatrix pEqn
          (
              fvm::laplacian(rAU, p) == fvc::div(phiHbyA)
          );

          pEqn.setReference(pRefCell, pRefValue);

          pEqn.solve(mesh.solver(p.select(piso.finalInnerIter())));

          if (piso.finalNonOrthogonalIter())
          {
              phi = phiHbyA - pEqn.flux();
          }
      }

      #include "continuityErrs.H"

      U = HbyA - rAU*fvc::grad(p);
      U.correctBoundaryConditions();
  }

}

// --- B-PISO loop
  while (bpiso.correct())
  {
      fvVectorMatrix BEqn
      (
          fvm::ddt(B)
        + fvm::div(phi, B)
        - fvc::div(phiB, U)
        - fvm::laplacian(DB, B)
      );
```

```
            BEqn.solve();

            volScalarField rAB(1.0/BEqn.A());
            surfaceScalarField rABf("rABf", fvc::interpolate(rAB));

            phiB = fvc::flux(B) + rABf*fvc::ddtCorr(B, phiB);

            while (bpiso.correctNonOrthogonal())
            {
                fvScalarMatrix pBEqn
                (
                    fvm::laplacian(rABf, pB) == fvc::div(phiB)
                );

                pBEqn.solve(mesh.solver(pB.select(bpiso.finalInnerIter())));

                if (bpiso.finalNonOrthogonalIter())
                {
                    phiB -= pBEqn.flux();
                }
            }

            #include "magneticFieldErr.H"
        }

        runTime.write();
    }

    Info<< "End\n" << endl;

    return 0;
}


// ************************************************************************* //
```